Reduced Order Modeling of Modal Coupling in Riveted Sandwich Beams

Jared Ashcraft[1], Matthew Ashcraft[2], Matthew S. Allen[3], and Brandon Rapp[4]

[1]Undergraduate Student, Brigham Young University, Department of Mechanical Engineering, jma279@byu.edu
[2]Undergraduate Student, Brigham Young University, Department of Mechanical Engineering, mca52@byu.edu
[3]Professor, Brigham Young University, Department of Mechanical Engineering, matt.allen@byu.edu
[4]Structures Engineer, Pratt & Whitney, brandon.rapp@prattwhitney.com

Abstract

Several recent studies have observed that, while quasi-linear modal models capture the behavior of jointed structures very well, nonlinear modal coupling is frequently observed. For example, a structure composed of two beams that are riveted along their lengths was recently shown to exhibit significant modal coupling in five of its first six modes [Gilbert et al. IMAC 2025]. Few studies have thoroughly characterized modal coupling in jointed structures, and the authors are not aware of any studies in which a model has been shown to accurately capture it. This paper explores whether this phenomenon can be captured by a reduced order model (ROM) in which the riveted joints are replaced by discrete Iwan elements. The model was previously optimized to reproduce the uncoupled modal behavior of the first mode and was shown to give a reasonable approximation of the uncoupled behavior of several other modes. In this study, the ROM is subjected to impulsive forces at various locations and simulated in the time domain to ascertain how it responds to inputs that excite the various modes to differing degrees. The results are compared to those obtained from impact testing of a prototype structure. Additionally, multi-mode quasi-static analysis is used to seek to predict bounds on the effective oscillation frequency and damping exhibited by each mode of interest when mode coupling is present.

Keywords: Nonlinear Joints, Iwan Element, Rivet, Modal Coupling

1 Introduction

Nonlinear modal coupling is often observed in structures [1, 2, 3, 4, 5], especially in the presence of mechanical joints such as rivets and bolts. Mechanical joints are probably the most common source of nonlinearity in assembled structures [6]. Uncoupled modal models have proven effective in many applications, for example as a basis for model updating [7, 8], to facilitate system identification [9] and to simplify modeling of nonlinear systems [10, 11, 12]. Nevertheless, even when a system can be well approximated as weakly nonlinear, nonlinear modal coupling can be encountered, making it difficult to predict or understand the response of the structure [5]. When modal coupling cannot be ignored, methods such as quasi-static modal analysis [13] or the single nonlinear resonant mode assumption [14, 15] are no longer applicable and so one must resort to more expensive analysis methods such as time integration [16] or harmonic balance [17]. Modal coupling occurs when multiple modes are excited simultaneously, causing interference that significantly affects the dynamic response of the structure.

A recent study [3] showed that a structure composed of two beams connected with 24 rivets along their lengths experienceed significant modal coupling for the first six modes, with the exception of the first bending mode. It was observed that the effective natural frequency and damping of most of the modes of the system changed as the impact location was varied, and this was attributed to modal coupling and the fact that different measurement points excite the modes to varying degrees. A companion study [18] reduced a finite element model (FEM) of the structure using interface spiders at each rivet and the Hurty/Craig-Bampton method [19, 20] and then replaced the riveted joints with discrete Iwan elements. They then used optimization and quasi-static analysis to find a reduced order model (ROM) of the structure that best reproduced the behavior of the first bending mode of the structure, which exhibited relatively little modal coupling. While their work thoroughly evaluated the ability of the ROM to capture the uncoupled modal behavior of the structure, modal coupling was not investigated.

The current work asks whether a ROM such as this can accurately predict and model the strong modal coupling that was observed in [3]. This coupling presumably occurs due to the nonlinear forces from each discrete joint, yet modeling the structure in this way assumes that one can neglect the details of the forces in each rivet and replace each with a discrete (nonlinear) Iwan

element. Time domain simulations of the full FEM of the structure would be quite computationally expensive, yet the ROM reduces the FEM to 333 DOF, so that time integration over several seconds can be performed in a matter of minutes-hours on a desktop computer. This study uses a variant on the ROM developed by [18] to simulate impact tests at various points as in the experiments [3]. The results are then compared with the experimental measurements to analyze the accuracy of the model in predicting modal frequencies and damping ratios as they shift due to modal coupling.

In addition to dynamic simulations, multi-mode quasi-static modal analysis (MM-QSMA) [21] was used in this work to predict bounds on the observed oscillation frequency and damping in the presence of modal coupling. The predictions were then analyzed and compared with the simulated test data to determine whether MM-QSMA can provide accurate bounds for frequency and damping on a sandwich beam subject to modal coupling.

2 Theory

The reduced order model of the riveted beam system described above uses discrete Iwan elements in place of the riveted joints. Iwan elements, originally developed by Iwan [22], are used to capture the nonlinear hysteretic behavior of built-up structures. They contain a distribution of Jenkins elements in parallel, which consist of a spring and a Coulomb friction slider. When experiencing a given load, only some of the Jenkins elements slip, which allows the Iwan elements to model nonlinear behavior like microslip. Segalman [23] created the four-parameter Iwan element used in this work. The four parameters are related to the stiffness of the joint and the force at which it slips completely.

In a previous work [18], a nonlinear model was created to simulate the response of the riveted sandwich beam mentioned above. First, a finite element model was made using spiders to constrain groups of nodes near each rivet to a single node, and then the model was reduced using the Hurty / Craig Bampton (HCB) method [24]. A Monte Carlo optimization procedure was then used to estimate the Iwan parameters that brought the model into agreement with measurements for the first bending mode. This optimization technique draws a uniform distribution of random samples from defined bounds around each of the parameters and repeats the process after tightening the bounds. Singh [25] extended the work of Lacayo [8] to develop the process that was used in [18]. Iwan elements were only applied in the x-direction (see Figure 1), and the Iwan parameters for all 24 rivets that hold the beam together were assumed to be the same. Figure 1 shows the location of the spiders along the length of the beam. Linear springs were used to join the 24 pairs of rivet nodes in the other directions. For more detailed information on how the ROM was created, see [18].

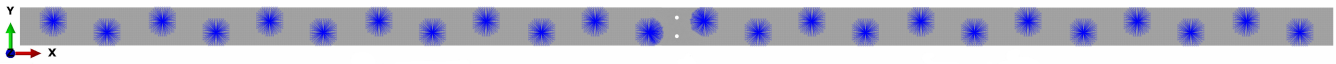

Figure 1: FEM model of the riveted beam showing the spiders that joined the mesh to a single node per rivet.

Once the parameters were optimized, the Iwan elements were used to predict the behavior of the beam using quasi-static modal analysis (QSMA). QSMA is a technique in which a force is applied that statically deforms a structure into the shape of one of its modes. The corresponding force-displacement curve is then used to construct a hysteresis loop, and thus to infer the effective vibration frequency and damping when the structure vibrates in only that mode [8]. The model found in [18] gave reasonable estimates of the damping ratios and natural frequencies of the first five bending modes. In the current work, these same methods were used to create an updated version of the ROM that included each of the drive points used in impact testing. This facilitated the simulation of impact tests, matching the testing conditions in [3].

In this work QSMA is first used to predict the uncoupled modal behavior when a single mode is excited. We also used an extension called MM-QSMA [21] as well as dynamic simulations to predict coupled modal behavior, which occurs when multiple modes are excited simultaneously. MM-QSMA uses the same principles as QSMA, but instead of deforming the beam into the shape of a single mode, it applies a force to deform the beam into a shape that is a superposition of two or more mode shapes. Singh et al. [21] used in-phase and out-of-phase linear combinations of two modes in MM-QSMA, and found that they produced conservative upper and lower bounds on the dynamic response of a finite element model. This study applies the MM-QSMA method from [21] to the riveted sandwich beam and presents new observations regarding its efficacy for complicated structures.

We processed the simulated time responses as was done in [3] filtering the data to isolate each mode and then using the Hilbert transform method to compute the frequency and damping for each mode. After filtering, the amlitude dependent natural frequencies and damping ratios for each mode were calculated and compared with the QSMA, MM-QSMA estimates, and impact test data.

The following sections discuss the ability of the ROM to capture the effects of modal coupling observed in the riveted beam

during impact tests and evaluate the potential of similar models to predict modal coupling in jointed structures.

3 Results

The purpose of this study was to determine how well a ROM that replaces riveted joints with discrete Iwan elements captures the effects of modal coupling and whether QSMA and MM-QSMA provide valuable insights to a beam's dynamic response. This section describes the results of the study and an analysis of how well these methods were able to predict the behavior of the system. Note that all the experimental data used in this section was collected in [3]. The following figure shows a section of the riveted sandwich beam with the location of the drive points (DP) used to excite both the physical beam and the ROM.

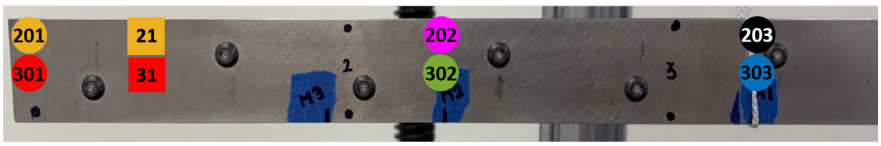

Figure 2: Locations of drive points used in empirical testing. The lines in Figures 12-16 are colored to match the corresponding drive point.

The beams have five bending modes in the frequency range of interest, which are denoted Mode B1 through Mode B5, and one torsion mode, which is denoted Mode T1. The beam also has axial modes and out-of-plane bending modes that were not observed in the test data. Drive points DP-203 and DP-303 were selected to suppress Mode B1, and points DP-202 and DP-302 were selected to suppress Mode B2, since they are located at the nodes of the modes they suppress (see Figure 4). The other points (DP-21, DP-31, DP-201, and DP-301) excited all of the bending modes in the frequency range of interest. The first three bending modes were tested at DP-21 and DP-31, and Mode B4 and Mode B5 were tested at DP-201 and DP-301. The drive points at the top of the beam were used to excite Mode T1 in addition to the bending modes.

3.1 QSMA

The ROM was used to test the accuracy of QSMA in predicting frequency and damping by running simulations of the dynamic response, with the initial condition of the beam being a deformation in the shape of one of the modes. This resulted in a response that almost purely excited the mode of interest. The resulting frequency and damping curves were found to closely match the QSMA prediction for each of the first five bending modes and the first torsion mode. Figure 3 shows the comparison of the Mode B3 QSMA with the pure Mode B3 dynamic response.

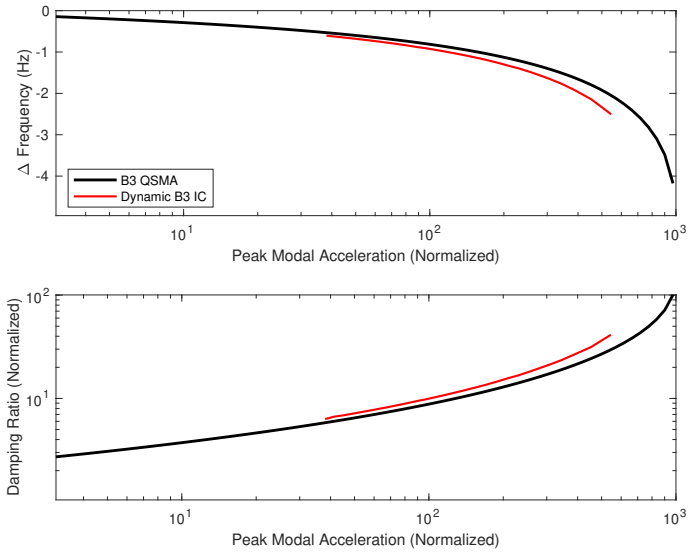

Figure 3: The dynamic simulation of the response of the beam when the initial condition is a displacement of the beam in the shape of Mode B3 and the QSMA prediction for that mode.

The curves show slight differences, which are thought to be either errors in the Hilbert Transform analysis, or slight inaccuracies in the time integration algorithm. This confirms previous findings [21, 18] that QSMA gives a fast and reasonable estimate of a beam's response when a single mode is excited. When multiple modes are excited simultaneously, MM-QSMA can be used to predict how much the frequency and damping may deviate from the uncoupled behavior [21], as described in the following subsection.

3.2 MM-QSMA

In contrast to the system studied in [21], the beams used in this study have free-free boundary conditions. A structure such as this has both symmetric and anti-symmetric modes, where the latter have a node at the center of the beam as shown in Figure 4.

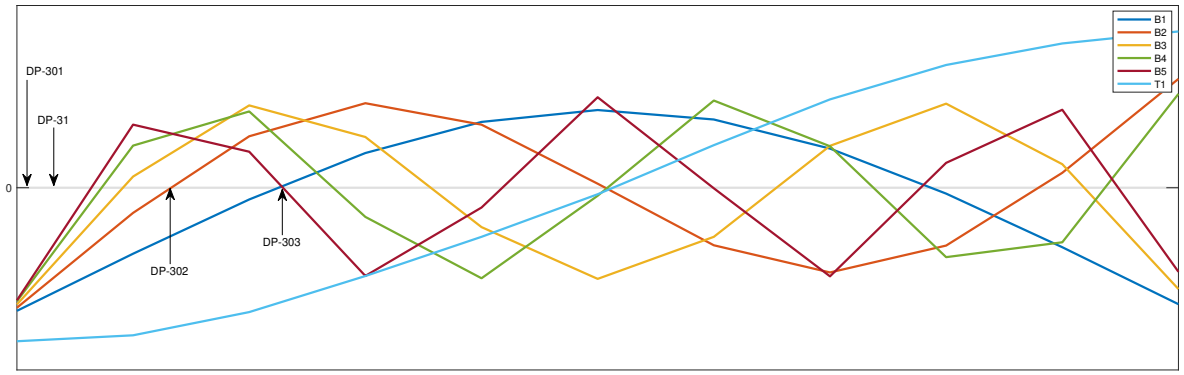

Figure 4: Mode shapes of the first five bending modes and the first torsion mode. Modes B1, B3, and B5 are symmetric, and Modes B2, B4, and T1 are anti-symmetric. The locations of the drive points in relation to the mode shapes are also represented.

When MM-QSMA was applied to this structure, we found that the results differed depending on whether the two superimposed modes were of the same type. Specifically, when a symmetric mode and an antisymmetric mode were combined, the results always predicted a decrease in frequency and an increase in damping, regardless of whether they were in or out-of-phase with each other. When both modes were of the same type, bounds were produced on both sides of the QSMA curve as was observed in [21]. For example, Figure 5 shows that the MM-QSMA of Mode B3 with Mode B1 provided upper and lower bounds for the response, since they were both symmetric modes. On the other hand, the MM-QSMA for Mode B3 and Mode B2 only resulted in bounds on one side of the QSMA curve since Mode B2 is anti-symmetric.

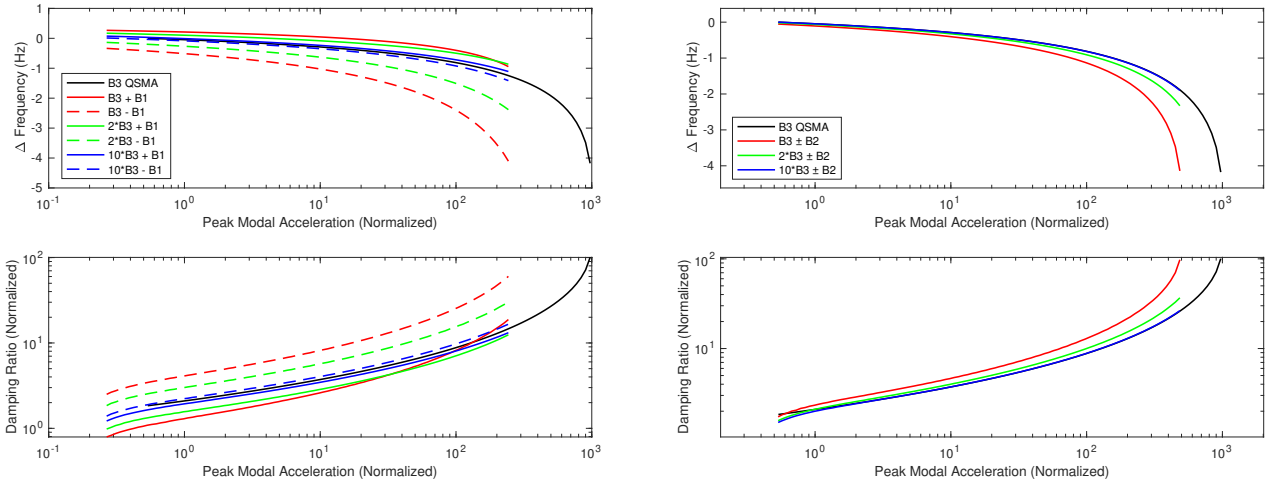

(a) (b)

Figure 5: (a) MM-QSMA predictions of frequency and damping for Mode B3 when it is perturbed by Mode B1. (b) MM-QSMA predictions when Mode B2 perturbs Mode B3. The different colors indicate the different ratios of the modes that were used.

MM-QSMA was also found to provide useful information that indicates which modes will have large coupling effects on other modes, as well as how modal coupling between those modes was likely to affect the frequency and damping of the system. The results of this study show that the amount of modal coupling is dependent on several factors, including which modes are being excited, the ratio of those modes to each other, and the amplitude of the response. MM-QSMA also predicts an increase in modal coupling as the peak modal acceleration increases, which explains some of the behavior seen in the impact testing from [3]. Work done to validate MM-QSMA is described in section 3.2.4.

3.2.1 Lower Mode Dominance

Moldenhauer [2] observed that modal coupling occurred between the first three bending modes of a structure to varying degrees; in his structure Modes 1 and 2 were not as affected as was Mode 3. The impact data used in this study [3] also showed that Mode B1 experienced minimal modal coupling when excited with other modes. MM-QSMA predicts this result, showing that when Mode B1 is combined with a higher mode, its frequency and damping are not significantly affected. On the other hand, Mode B1 has a significant impact on both the frequency and damping of the higher modes. This can be observed in Figure 6 which shows the difference between the MM-QSMA predictions for combinations of Modes B1 and B5.

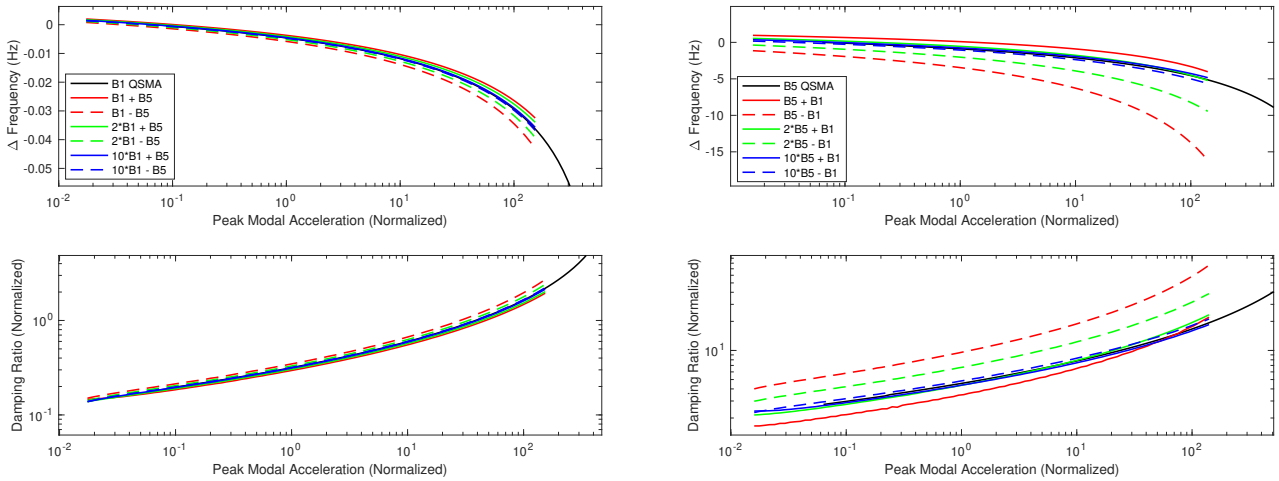

(a) (b)

Figure 6: Frequency and damping versus amplitude predicted by MM-QSMA when Mode B5 perturbs Mode B1 and vice versa. (a) Results for Mode B1. (b) Results for Mode B5.

When Mode B1 is combined with Mode B5, MM-QSMA predicts very little shift in frequency, as shown in Figure 6a. The widest MM-QSMA bound stays within 0.01 Hz of the pure Mode B1 QSMA curve over the included range of peak modal accelerations. On the other hand, Figure 6b shows that Mode B5 has significant shifts in frequency. The widest MM-QSMA bound deviates from the Mode B5 QSMA by over 11 Hz at the highest modal acceleration shown. The damping for Mode B1 is also much less affected than is the damping of Mode B5. Similarly, while the results are not shown here, MM-QSMA also predicted that Mode B2 would have a relatively large effect on the higher modes, but the effect of higher modes on Mode B2 was significantly smaller. This indicates that most modal coupling is caused by the lower bending modes for this structure. The dynamic responses shown in Sec. 3.3 confirm these findings.

3.2.2 MM-QSMA with the First Torsion Mode

MM-QSMA was also applied between the first torsion mode and the other modes. MM-QSMA predicted that Mode T1 would be affected by the other bending modes, but that Mode B1-B5 would not be affected by Mode T1. For example, the frequency and damping of the first bending mode appear to be unaffected by the presence of Mode T1, as seen in Figure 7, but both the frequency and damping of Mode T1 are shifted significantly by Mode B1.

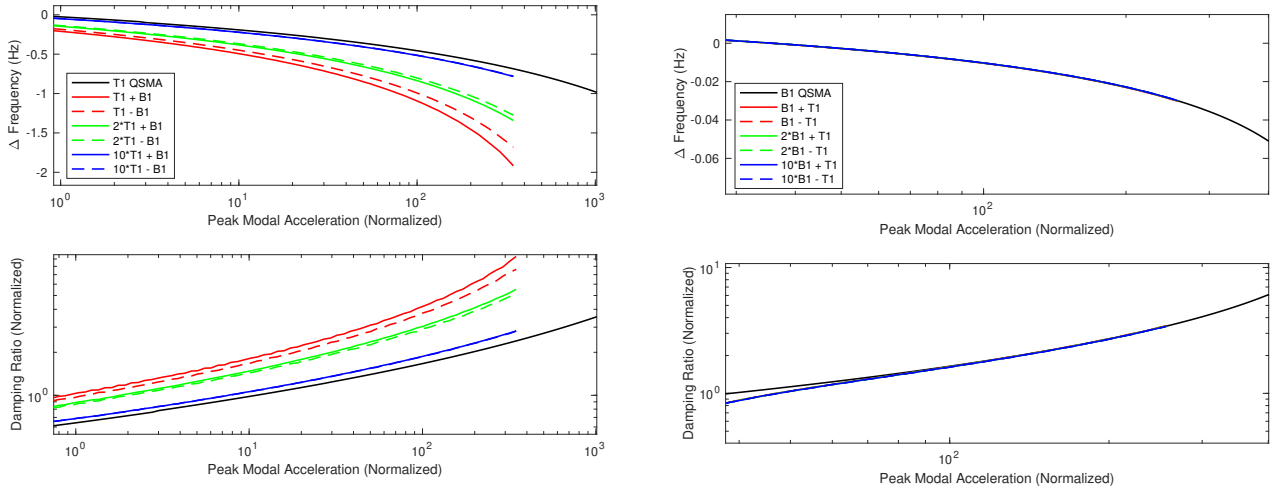

(a) (b)

Figure 7: (a) MM-QSMA curves showing the effect of Mode B1 on Mode T1. (b) MM-QSMA curves showing the effect of Mode T1 on Mode B1.

While not shown here for brevity, the MM-QSMA predictions for the frequency and damping of the other bending modes showed that they were unaffected by the presence of Mode T1. This indicates that the presence of the torsion mode can be ignored when analyzing the bending modes, but the bending modes are important to consider when analyzing the torsion mode.

The physical data also seems to agree with these findings. For example, Figure 13 shows the physical data for Mode B2. The red and yellow lines correspond to impulses applied at DP-31 and DP-21. DP-21 excites Mode T1 in addition to all the modes excited at DP-31. The data for DP-31 and DP-21 deviates more from the uncoupled behavior (Impulses at DP-303) as the magnitude of the impulse force increases, but there are no systematic differences between the data at DP-31 and DP-21.

3.2.3 MM-QSMA with 3 Modes

This study also expanded MM-QSMA to use a combination of three mode shapes to see if it could provide a better prediction of the response caused by an impulse force that excites a large number of modes at various amplitudes. Adding a third mode to MM-QSMA was found to slightly shift the frequency and damping estimates of the mode of interest, as can be seen in Figure 8.

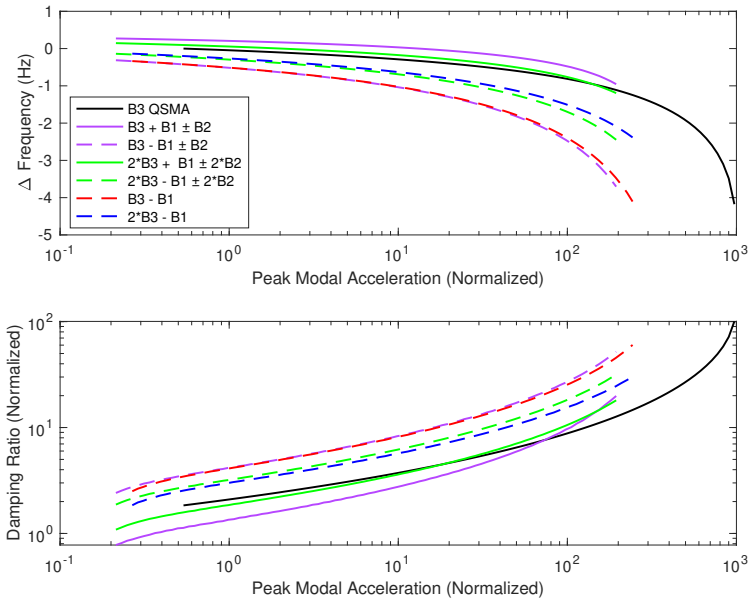

Figure 8: The MM-QSMA prediction for bending Mode B3 coupled with both Mode B1 and Mode B2

An impulse force often excites even more than three modes in the beam, but in this case, adding Mode B2 did not provide a notable change in the prediction, since Mode B1 has a much stronger effect on Mode B3. Although including more modes in MM-QSMA process may increase the accuracy of the predicted bounds, it also adds more complexity, so this method was not pursued further. Instead, we used MM-QSMA to analyze the mode of interest coupled with the bending mode that was the most prominent in the impulse response.

3.2.4 Validating MM-QSMA

To validate the predictions resulting from MM-QSMA, we used dynamic simulations with initial conditions being the displacement of the beam in the shape of combinations of multiple modes. We compared these dynamic responses with the MM-QSMA curves resulting from the same combinations of modes.

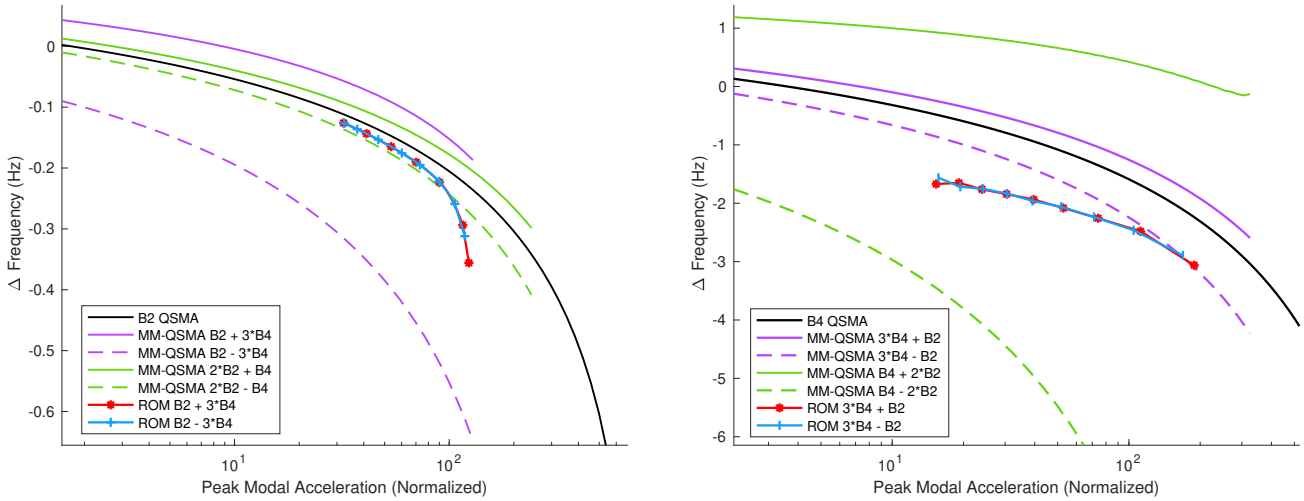

(a) (b)

Figure 9: Dynamic simulation frequency results for combining Mode B2 with 3*B4 in- and out-of-phase with corresponding MM-QSMA curves. (a) Results for Mode B2. (b) Results for Mode B4.

Figure 9 shows the comparison between a dynamic response, with an initial displacement being a 1:3 ratio of the shapes of Mode B2 to Mode B4, and MM-QSMA. The highest peak modal accelerations correspond to the beginning of the simulation. Thus, the frequencies for Modes B2 and B4 begin within the MM-QSMA bounds with a 1:3 ratio (purple lines). As the time simulation progressed (shown by the decreasing modal acceleration), Mode B4 dies out much more quickly than Mode B2. The dynamic response of Mode B2 remains within the bounds formed by the initial ratio of modes as Mode B2 becomes more and more dominant over time, approaching the QSMA prediction for pure Mode B2. However, the result for Mode B4 leaves the bounds of the initial MM-QSMA prediction as the ratio of B4:B2 decreases. Thus, an updated MM-QSMA prediction can be used to estimate the dynamic response more accurately to reflect the changing ratio. When using a 2:1 ratio between Mode B2 and Mode B4 (green lines), the MM-QSMA bounds remain conservative for Mode B4 and also provide tighter bounds on the estimate for Mode B2 as the simulation reaches lower modal accelerations.

Interestingly, although MM-QSMA predicted upper and lower bounds for the response shown in Figure 9, the dynamic simulation resulted in roughly the same frequency and damping curves, regardless of whether the modes were added or subtracted. Both showed a decrease in frequency and an increase in damping in the response compared to the QSMA curve. The lack of difference is due to the fact that the two modes have different frequencies and move in- and out-of-phase over time. MM-QSMA calculates the response as if the modes remain strictly in-phase or out-of-phase, as defined by the initial condition. Although this decreases the accuracy of the prediction, it also ensures that the estimate is conservative for a given ratio of modes.

These observations demonstrate that MM-QSMA provides helpful predictions for the effects of modal coupling at computation speeds that are significantly faster than dynamic simulations. For example, the dynamic simulation data in Figure 9a, which simulated the first 5 seconds of the response, each took approximately 156 times longer than was needed to produce the five QSMA and MM-QSMA curves (roughly 31 times longer per second of simulated data). For tests that excite Mode B1, longer simulations are necessary to capture the full response, since Mode B1 requires more time to decay.

Although MM-QSMA is much faster than dynamic simulations, additional testing and analysis are necessary for situations that require higher levels of precision and accuracy. The size of the bounds that result from MM-QSMA is dependent on the ratio

of the modes that are present, and accurate predictions depend on the use of reasonable estimates for that ratio. Thus, it is important to consider the change in the amplitude ratios between modes over the course of the response.

3.3 Dynamic Simulations

This section describes the results of the dynamic simulations and how well the model was able to match the trends seen in the experimental data collected in [3]. The impulse for each dynamic simulation was approximated using a half sine wave with an amplitude equal to the maximum impulse force of the corresponding experimental test. Experimental impact testing was performed with two different hammers depending on the desired bandwidth of the impulse force. Most of the tests were performed with a medium-sized hammer. The hammer data was not sampled with sufficient resolution to resolve the impulse with high accuracy, so it could not be used directly as an input force in the simulations. Hence, all input forces were approximated as sinusoidal pulses with the same frequency. The mean pulse frequency of the experimental tests using the medium hammer was found to be 270 Hz with a standard deviation of 40 Hz. As can be seen in Figure 10, changing the pulse frequency within two standard deviations of the mean did not have a significant effect on the response, so the average frequency was used for each of the dynamic simulations.

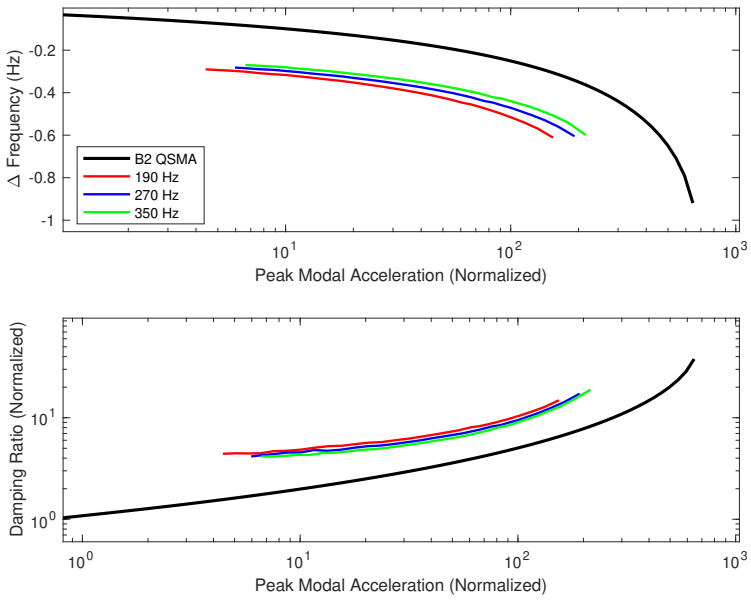

Figure 10: Dynamic simulations for Mode B2 varying the pulse frequency within two standard deviations of the sample mean. All three tests were performed with a force of 62 N applied at DP-31.

Impact tests for Modes B4, B5, and T1, which required a higher pulse frequency to be excited, were performed with a different hammer. These impacts had an average pulse frequency of 2040 Hz. This frequency was used for the corresponding dynamic simulations.

3.3.1 Comparing Dynamic Simulations with MM-QSMA

Comparing the prediction of MM-QSMA with the impulse data simulated by the ROM is difficult, both because an impulse excites many of the modes and because the ratio of the strength of each mode changes with time as the higher modes die out faster than the lower ones. However, the comparison can provide valuable insights. Figure 11 gives an example of the comparison between MM-QSMA and two dynamic simulations.

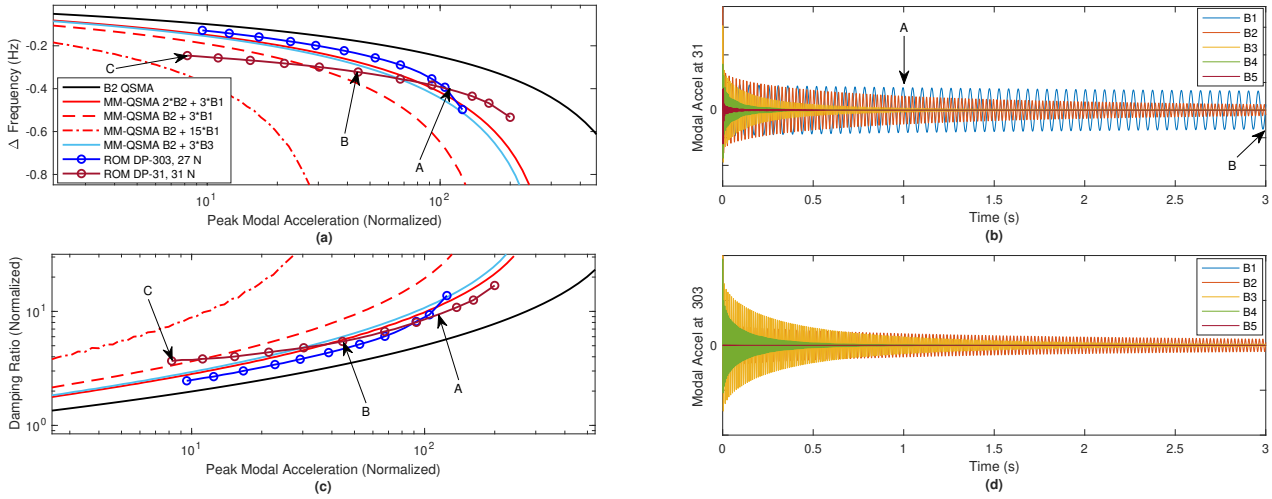

Figure 11: (a) MM-QSMA frequency prediction and frequency of dynamic responses for Mode B2. (b) Modal acceleration of each mode over time for the 31 N impulse at DP-31. (c) MM-QSMA damping prediction and damping from dynamic responses for Mode B2. (d) Modal acceleration of each mode over time for the 27 N impulse at DP-303. Markers A, B, and C correspond to certain times and ratios B1:B2 in the response of the impulse at DP-31 as described in Table 1.

The impulse at DP-31 excites all the bending modes, but the higher modes decay quickly, and the response soon becomes mainly a combination of Mode B1 and Mode B2 as shown in Figure 11b. The ratio between Modes B1 and B2 changes throughout the response as Mode B1 becomes increasingly dominant. Markers A, B, and C correspond to the times and ratios (B1:B2) shown in Table 1 and mark the corresponding points along the frequency and damping curves for the impulse at DP-31 in Figure 11a and Figure 11c. Note that as the ratio B1:B2 changes, the response always remains within the MM-QSMA bounds corresponding to that ratio. For example, at the end of the 9 second simulated response, the amplitude ratio is about 15:1, and Figure 11a and Figure 11c show that, while the frequency and damping at this time exceeds the bound of the 3:1 MM-QSMA curve, it is well within the 15:1 bound.

Table 1: This table defines the times corresponding to the markers A, B, and C in Figure 11, as well as the approximate ratio of the strengths of the Modes B1 and B2 at those points in the DP-31 response.

Marker	Time (s)	Ratio B1:B2
A	1	3:2
B	3	3:1
C	9	15:1

On the other hand, most of the interaction between modes in the impulse at 303 is between Mode B2 and Mode B3 as shown in Figure 11d. The beginning of the response (the highest peak modal acceleration) for the impulse at DP-303 has a ratio B2:B3 of approximately 1:3, and the response fits within the MM-QSMA bounds with that ratio, as shown in Figure 11 a and 11c. As the peak acceleration decreases, all other modes apart from Mode B2 decay quickly, causing the frequency and damping to move closer to the pure mode 2 prediction from QSMA. Thus, the entire response remains within the initial 1:3 ratio of Mode B2 to B3.

This example demonstrates that MM-QSMA gives useful predictions of the frequency and damping at specific times in the response when ratios of the mode of interest with the most dominant mode are known.

3.3.2 Bending Modes

The low-order bending modes take much longer to decay than the high bending modes after an impulse. Because of this, the lower bending modes cause a significant amount of modal coupling in the higher bending modes, and an increasing amount of modal coupling, shown by large shifts in frequency and damping, seems to occur as the modes increase in order.

For example, the first bending mode exhibits considerably less modal coupling than each of the other modes. This is shown by the lack of spread between the experimental data, as well as the minimal shift in the simulated dynamic responses from the

Mode B1 QSMA curve.

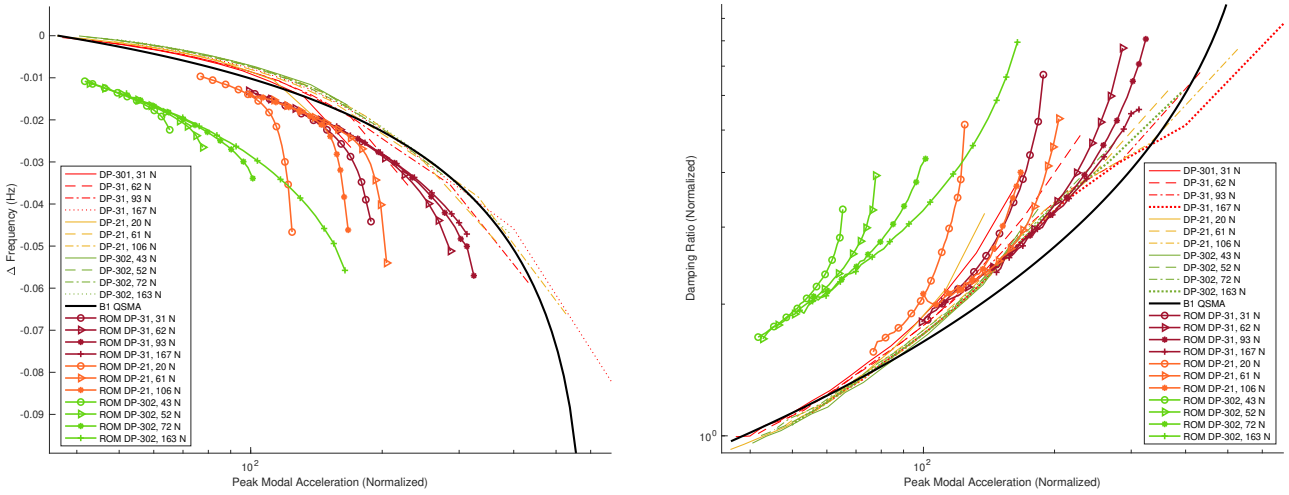

(a) Mode B1 Frequency

(b) Mode B1 Damping

Figure 12: Mode B1 frequency and damping plots showing the QSMA prediction, the impact data, and the dynamic response from the ROM.

As can be seen in Figure 12, the simulated responses approach the QSMA curve as the peak modal acceleration decreases. This is because the response of the impulse begins with the excitation of many modes, but these all decay rapidly relative to Mode B1. Thus, as time passes, the system approaches a pure Mode B1 response. This can be seen by how the ROM simulations converge towards the Mode B1 QSMA prediction as peak modal acceleration decreases. It is interesting to note that the simulations at DP-302 appear to converge to a slightly different curve than the impulses at the other points. The reason for this is not yet known.

Overall, Mode B1 exhibits minimal variation in frequency and damping, having a similar response regardless of the initial force and location of the impulse. This implies that Mode B1 experiences little modal coupling since its behavior is not significantly affected by the presence of the other modes. In contrast, Mode B2 had much more significant shifts in both frequency and damping as shown in Figure 13.

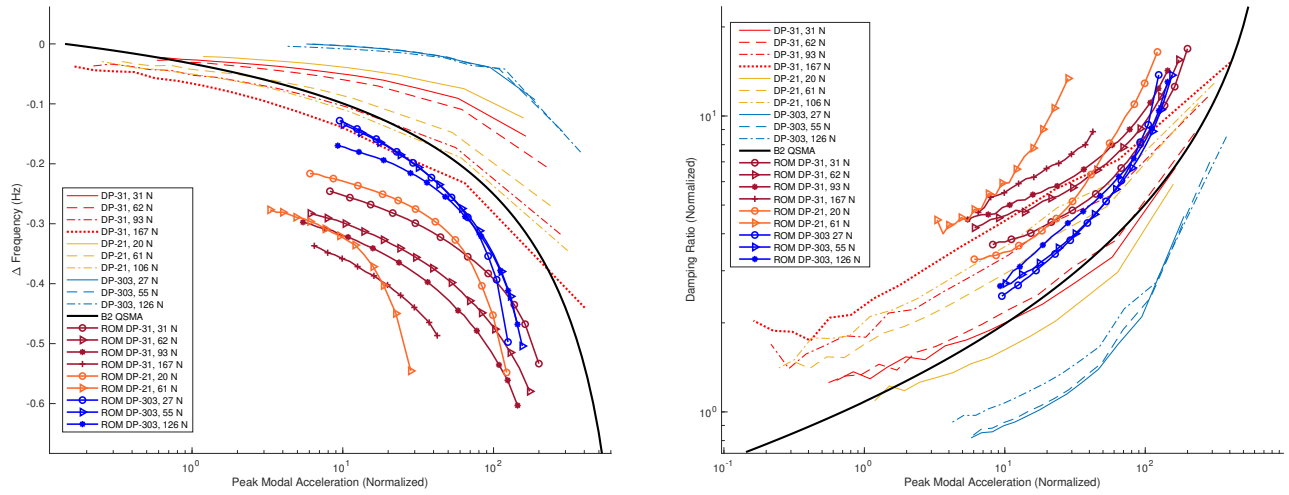

(a) Mode B2 Frequency

(b) Mode B2 Damping

Figure 13: Mode B2 frequency and damping plots showing the QSMA prediction, the impact data, and the dynamic response from the ROM.

The experimental data shows that Mode B2 experiences the lowest shifts in damping and frequency for DP-303 compared to DP-21 and DP-31. This is because DP-303 is at the node of the first bending mode, and an impulse there suppresses Mode B1. This causes Mode B2 to be the dominant mode, since all the other modes that are excited to a significant amplitude decay much more rapidly than Mode B2. Note that the ROM perfectly agrees with these trends, except that the curves are shifted relative to the experimental data. The ROM does not fit the data extremely well for Mode B2; presumably the behavior when B2 is isolated should have a smaller frequency shift and lower damping than the data for impacts at DP-303. As was noted previously, the ROM was tuned for Mode B1 and this mismatch in Mode B2 resulted. Additional research could determine whether a single ROM could be tuned to capture both Modes B1 and B2 with higher fidelity.

Another evidence of modal coupling from [3] was that applying different magnitudes of force at the same drive point causes both frequency and damping of the mode of interest to shift. Harder impact forces were observed to cause higher damping and larger downward shifts in frequency for all of the modes except for Mode B1. The ROM was tested to see if it could capture this behavior. The results of those tests for the second bending mode are shown in Figure 14.

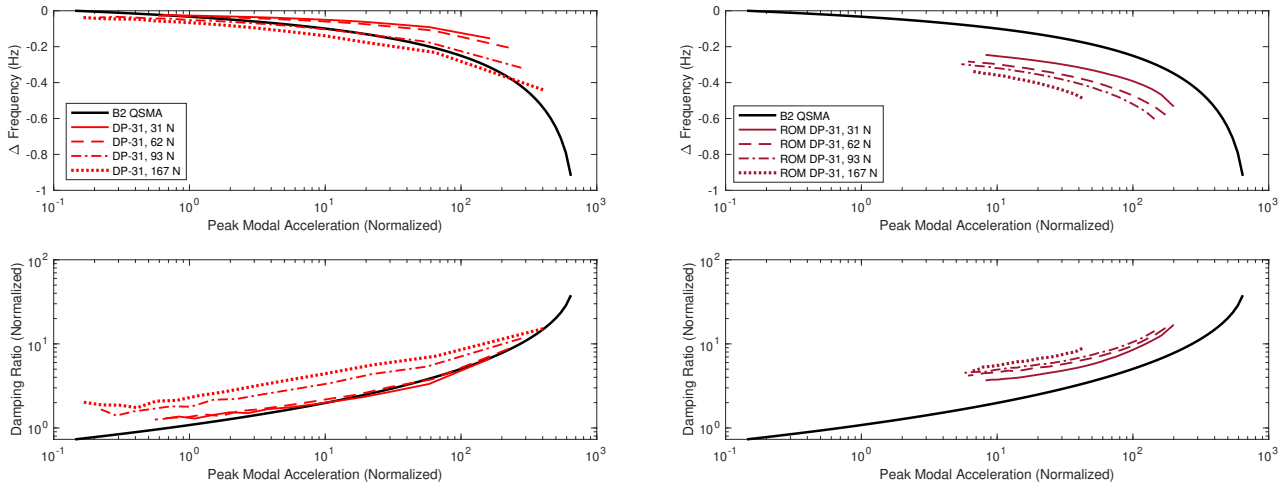

(a) (b)

Figure 14: (a) Experimental data for Mode B2 with varied forces applied at DP-31. (b) Simulated impulse responses at DP-31 with the same varied forces applied. The Mode B2 QSMA is included for reference.

As can be seen in this figure, the ROM is successful at reproducing the shift in damping and frequency due to varied impulse forces. This shows that as the force imparted to the structure increases, Mode B2 deviates more and more from the frequency and damping than it would have if it were excited in isolation. The same was observed for Modes B3, B4 and B5.

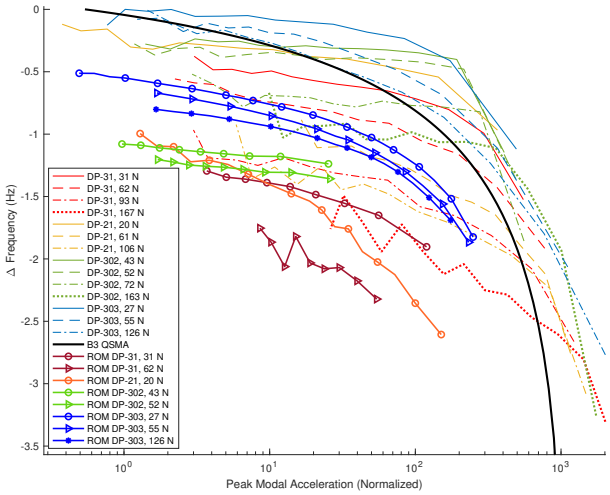

(a) Mode B3 Frequency

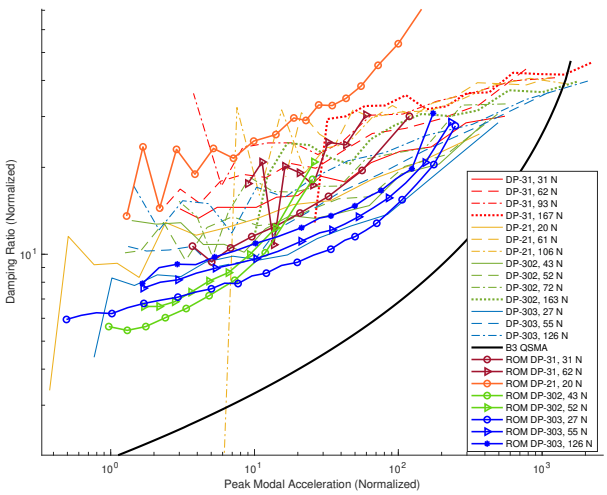

(b) Mode B3 Damping

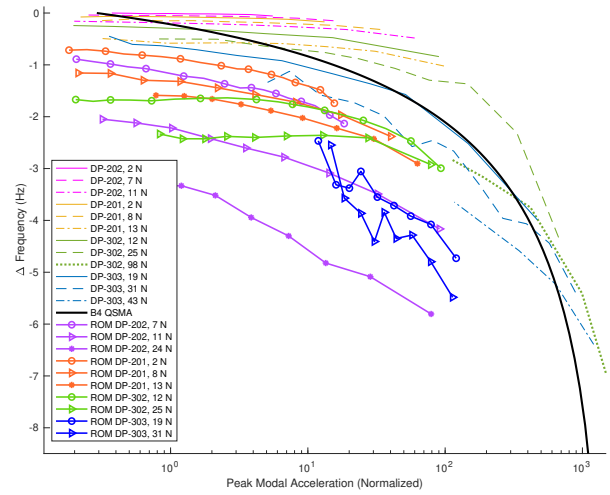

(c) Mode B4 Frequency

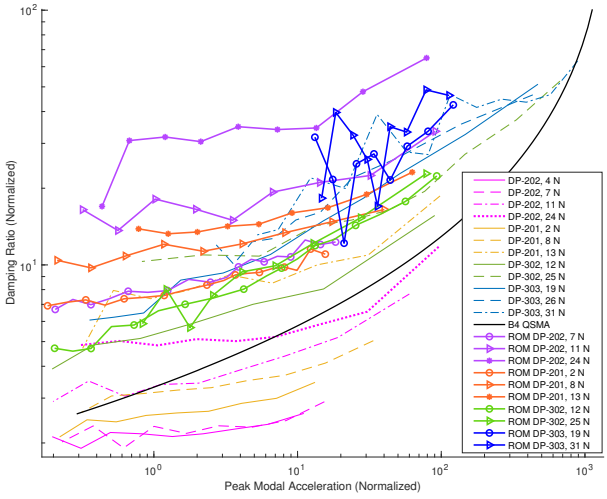

(d) Mode B4 Damping

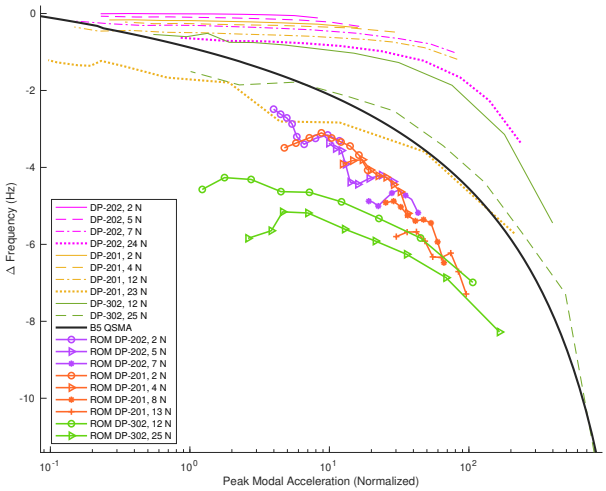

(e) Mode B5 Frequency

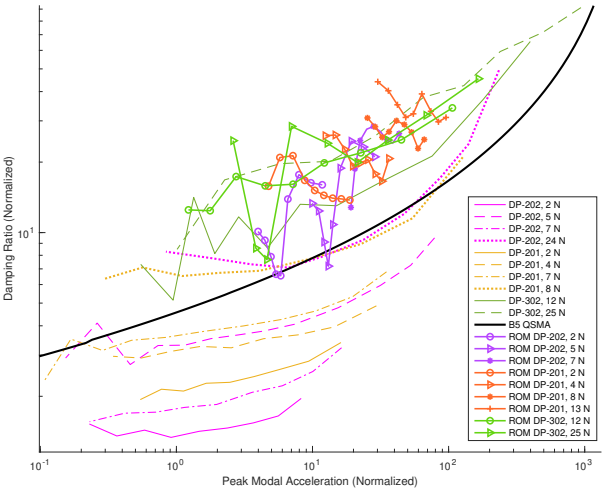

(f) Mode B5 Damping

Figure 15: Frequency and damping plots for Modes B3, B4, and B5 showing the QSMA prediction, the impact data, and the dynamic response from the ROM.

When an impulse was applied, the higher modes were observed to experience larger effects from modal coupling. Figure 15 shows the results of the dynamic simulations of Modes B3, B4, and B5, in addition to the experimental data from [3]. Similarly to what was observed with Mode B2, Mode B3 exhibited an increasing amount of modal coupling as larger impulse forces were applied at a given drive point. There is also less modal coupling at DP-303, where Mode B1 is suppressed; Figures 15a and 15b show that for Mode B3, impulses applied at DP-303 produce minimal spread in the frequency and damping, causing them to be close to the single-mode QSMA prediction.

The time simulations from the ROM for Modes B4 and B5 have a spread comparable to that of the impact data in both frequency and damping. However, the ROM is not as consistent in following the trends in the experimental data for these modes. Because they decay very quickly after an impulse and are only present when there are significant effects from the lower bending modes, the dynamic responses for these modes were difficult to capture. In particular, band-pass filtering and the Hilbert transform were used to post process the dynamic responses to extract the frequency and damping of each mode as a function of time. This process can introduce larger errors when a mode decays very quickly, and this is thought to be the cause of the irregularity in the data from the simulations.

In any event, Modes B4 and B5 show quite large deviations from the behavior that each would have if excited in isolation, and the ROM does at least capture the magnitude of these variations. For example, the data shows that Mode B4 shows about a factor of 10 increase in damping at an acceleration of 10 (normalized), relative to the minimum damping, and the model shows an 8-9 times increase in damping at the same peak modal acceleration relative to the QSMA prediction of the uncoupled behavior. On the other hand, the model does not precisely predict the amount of modal coupling observed from each drive point.

Overall, the impulse responses simulated using the ROM agree with the physical data in that modal coupling lowers the natural frequency and increases the damping in the beam. These results show that simulations of impacts on the model follow expected trends and give reasonable estimates of frequency and damping for the first five bending modes. This provides further confidence in the model's ability to predict the behavior of the structure in an arbitrary environment, in which many modes may be excited simultaneously.

3.3.3 First Torsion Mode

In [18], it was found that the ROM was unable to accurately predict the behavior of the first torsion mode. It significantly underestimated the level of nonlinearity in the natural frequency at the modal accelerations that were tested, and the damping ratio was under-predicted by more than an order of magnitude. Figure 16 shows that the shift in the frequency and damping predicted by the ROM due to modal coupling are also far lower than those observed experimentally.

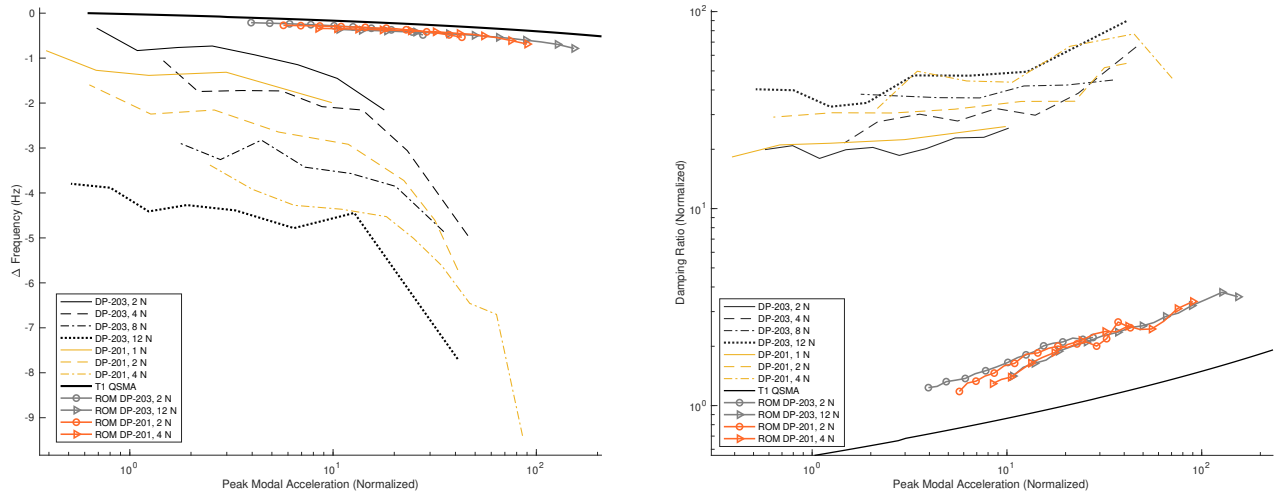

(a) Mode T1 Frequency

(b) Mode T1 Damping

Figure 16: Frequency and damping plots for Mode T1 showing the QSMA prediction, the impact data, and the dynamic response from the ROM.

The dynamic responses show very little modal coupling in this mode, but the experiments have significant variation in the measurements for frequency and damping. Further research is needed to understand why this torsion mode is not accurately

captured. Tests are underway on similar structures with different lengths and rivet spacing, to see if the torsion mode is always captured poorly or whether this is a fluke for this one particular structure.

4 Conclusion

This study explored the extent to which the effects of modal coupling that occur in jointed structures could be accurately captured using a reduced-order model. The ROM used was optimized to follow the uncoupled behavior of Mode B1, and impact tests were simulated using the ROM and compared to the physical data reported in [3]. The results show that, for the structure studied here, the ROM gives good estimates of the frequency and damping observed for various modes after an impulse is applied to the structure. This study only considered a single prototype riveted sandwich beam, but one would hope that the results would generalize to other structures with similar characteristics.

The ROM was found to correctly predict the trends of changes in frequency and damping with respect to both the location and the magnitude of an applied impulse force. It accurately showed that the affects of modal coupling increased as the strength of the impulsive forces increased; both the ROM and the data show that the frequency and damping deviated more from the uncoupled behavior (i.e. that the modal coupling was more severe) as the magnitude of the impulse increased. It is not clear why this would be the case. An increase in the force level should increase the amplitude of each mode by similar amounts, so the ratios of their response amplitudes should remain similar. This should be further explored, as the simulations from the ROM provide one with a detailed view of what is happening inside each Iwan element.

Although the model fails to accurately capture the first torsion mode, the insights gained by analyzing the other modes can still help to explain some of the behaviors observed in the impact test data. For example, the same pattern of increasing shifts in frequency and damping as larger forces were applied was also observed in the data for Mode T1.

As noted in [18], the ROM was tuned to capture the behavior of Mode B1, and it does not happen to exactly reproduce the behavior of the other bending modes. Considering that, it is encouraging to see how well it captures the modal coupling that was observed in the experimental measurements. A different optimization method could improve the accuracy of the model by allowing the model to be optimized to match both Mode B1 and Mode B2.

A previous study using MM-QSMA applied the technique to simple beams with one or two mechanical joints [21]. The current work applied this technique to a more complex structure with 24 joints and found that MM-QSMA can predict bounds for the response due to modal coupling and is a computationally efficient way to obtain a good estimate for changes in frequency and damping caused by modal coupling, even in this complicated structure.

MM-QSMA was also shown to be a useful tool for gaining a better understanding of the interactions between modes and which modes are likely to change their behavior when other modes are excited along with them. For example, when combining symmetric and anti-symmetric modes in MM-QSMA, it only predicted a decrease in the frequency and an increase in damping, while combining two modes of the same type produces bounds on both sides of the QSMA curve. Interestingly, the dynamic simulations always showed the same pattern of decreasing frequency and increasing damping. This suggests that it may not be necessary to calculate both sides of the bounds.

The bounds predicted by MM-QSMA depend on the ratio of the strengths of the excited modes. Because the modes decay at different rates after an impulse on the beam, MM-QSMA cannot give a prediction for the whole response at once. However, it can give predictions for times when the ratios of the strengths of the modes can be estimated.

The success of this model in capturing the effects of modal coupling shows that the methods used can effectively predict modal coupling in jointed structures. Future works would benefit from having more data that covers a larger range of modal amplitudes, which would allow the ROM to be more finely tuned, leading to a more accurate model. Other filtering and processing methods could also be considered to more accurately capture the behavior of Modes B4, B5, and T1.

References

[1] Guillaume Fritz, Jean-Jacques Sinou, Jean-Marc Duffal, and Louis Jézéquel. Investigation of the relationship between damping and mode-coupling patterns in case of brake squeal. *Journal of Sound and Vibration*, 307(3):591–609, 2007.

[2] Benjamin J. Moldenhauer, Aabhas Singh, Phil Thoenen, Daniel R. Roettgen, Benjamin R. Pacini, Robert J. Kuether, and Matthew S. Allen. Influences of Modal Coupling on Experimentally Extracted Nonlinear Modal Models. In Gaetan Kerschen, M. R. W. Brake, and Ludovic Renson, editors, *Nonlinear Structures and Systems, Volume 1*, Conference

Proceedings of the Society for Experimental Mechanics Series, pages 189–204, Orlando, FL, January 2019. Springer International Publishing.

[3] Suzanna Gilbert, Matthew S. Allen, and Brandon Rapp. Nonlinear System Identification of a Riveted Beam using a Hilbert Transform Based Approach. In *Proceedings of IMAC XLIII*, Orlando, Florida, February 2025.

[4] Mitchell P. J. Wall, Allen Allen, Matthew S, and Robert J. Kuether. Observations of Modal Coupling due to Bolted Joints in an Experimental Benchmark Structure. *Mechanical Systems and Signal Processing*, 162:107968, 2022.

[5] Matt Griebel, Adam Johnson, Brent Erickson, Joel Sills, and Matthew S. Allen. Orion MPCV Nonlinear Dynamic Correlation and Model Updating using Quasi-Static Modal Analysis. El Segundo, CA, June 2021. Matt Griebel, Adam Johnson, Brent Erickson, Quartus Engineering, Inc., Paul Bremner, AeroHydroPLUS, Joel Sills, NASA Engineering Safety Center.

[6] C Beards. Damping in Structural Joints. *The Shock and Vibration Digest*, 11(9):35–41, 1979.

[7] Matthew S. Allen, Joseph D. Schoneman, Wesley Scott, and Joel W. Sills. Application of Quasi-Static Modal Analysis to an Orion Multi-Purpose Crew Vehicle Test. Houston, Texas, February 2020.

[8] Robert M. Lacayo and Matthew S. Allen. Updating Structural Models Containing Nonlinear Iwan Joints Using Quasi-Static Modal Analysis. *Mechanical Systems and Signal Processing*, 118(1 March 2019):133–157, 2019. Number: 1 March 2019.

[9] Mengshi Jin, Matthew R. W. Brake, and Hanwen Song. Comparison of nonlinear system identification methods for free decay measurements with application to jointed structures. *Journal of Sound and Vibration*, 453:268 – 293, 2019.

[10] M. Krack, L. Panning-von Scheidt, and J. Wallaschek. A method for nonlinear modal analysis and synthesis: application to harmonically forced and self-excited mechanical systems. *Journal of Sound and Vibration*, December 2013.

[11] Malte Krack. Nonlinear modal analysis of nonconservative systems: Extension of the periodic motion concept. *Computers & Structures*, 154:59–71, July 2015. extended periodic motion concept EPMC.

[12] Nidish Narayanaa Balaji and Matthew R.W. Brake. A quasi-static non-linear modal analysis procedure extending Rayleigh quotient stationarity for non-conservative dynamical systems. *Computers & Structures*, 230:106184, April 2020.

[13] Robert Lacayo, Luca Pesaresi, Johann Gross, Daniel Fochler, Jason Armand, Loic Salles, C. W. Schwingshackl, Matthew S. Allen, and Matthew R. Brake. Nonlinear modelling of structures with bolted joints: a comparison of two approaches based on a time-domain and frequency-domain solver. *Mechanical Systems and Signal Processing*, 114,(1 January 2019):413–438, 2019.

[14] W. Szemplińska-Stupnicka. The modified single mode method in the investigations of the resonant vibrations of non-linear systems. *Journal of Sound and Vibration*, 63(4):475 – 489, 1979.

[15] Malte Krack. Extension of the single-nonlinear-mode theory by linear attachments and application to exciter-structure interaction. *Journal of Sound and Vibration*, 505:116120, 2021.

[16] Wolfgang Witteveen, Michael Kuts, and Lukas Koller. Can transient simulation efficiently reproduce well known nonlinear effects of jointed structures? *Mechanical Systems and Signal Processing*, 190:110111, May 2023.

[17] Krack, Malte and Gross, Johann. *Harmonic Balance for Nonlinear Vibration Problems*. Mathematical Engineering. Springer Cham, 2019.

[18] Blackham, Joshua, Stoker, Cameron, Allen, Matthew S., and Rapp, Brandon. Nonlinear Model Updating for Riveted Joints. In *Proceedings of the 43rd International Modal Analysis Conference*, Orlando, FL, February 2025.

[19] W. C. Hurty. Dynamic analysis of structural systems using component modes. *AIAA Journal*, 3(4):678–685, April 1965. Number: 4.

[20] R. R. Jr. Craig and M. C. C. Bampton. Coupling of Substructures Using Component Mode Synthesis. *AIAA Journal*, 6(7):1313–1319, 1968. Number: 7.

[21] Singh, Aabhas, Allen, Matthew S., and Kuether, Robert J. Multi-mode Quasi-static Excitation for Systems with Nonlinear Joints. *Mechanical Systems and Signal Processing*, Vol. 185(15 February):109601, 2023.

[22] W. D. Iwan. A Distributed-Element Model for Hysteresis and Its Steady-State Dynamic Response. *Journal of Applied Mechanics*, 33(4):893–900, December 1966.

[23] Daniel J. Segalman. A Four-Parameter Iwan Model for Lap-Type Joints. *Journal of Applied Mechanics*, 72(5):752–760, February 2005.

[24] Aabhas Singh, Wall, Mitchell, Allen, Matthew S., and Kuether, Robert J. Spider Configurations for Models with Discrete Iwan Elements. In *Nonlinear Structures and Systems*, volume 1, pages 25–38, Orlando, Florida, January 2019. Springer.

[25] Aabhas Singh, Matthew S. Allen, and Robert J. Kuether. Multi-mode Quasi-static Excitation for Systems with Nonlinear Joints. Orlando, Florida / Virtual, February 2021.